
Article:
Chen, X. and Wang, J. (2017) Magnetomotive force harmonic reduction techniques for fractional-slot non-overlapping winding configurations in permanent-magnet synchronous machines. Chinese Journal of Electrical Engineering, 3 (2). pp. 102-113. ISSN: 2096-1529

https://doi.org/10.23919/CJEE.2017.8048416

Magnetomotive Force Harmonic Reduction Techniques for Fractional-Slot Non-Overlapping Winding Configurations in Permanent-Magnet Synchronous Machines

Xiao Chen, and Jiabin Wang*

(Department of Electronic and Electrical Engineering, University of Sheffield, Sheffield, S3 7HQ, UK)

Abstract: Compared to conventional distributed winding configurations, the fractional-slot non-overlapping (concentrated) windings exhibit advantages such as short end-winding length, high copper packing factor (particularly with segmented stator structure), low cogging torque, good field weakening capability owing to relatively large d-axis inductance, and better fault tolerant capability due to low mutual inductance. However, one of the key problems of employing concentrated windings in Permanent-magnet Synchronous Machines(PMSMs) is the high eddy-current losses in rotor magnets and/or rotor iron due to the presence of a large number of lower and higher order space harmonics in the stator Magneto-Motive Force(MMF). These MMF harmonics also result in other undesirable effects, such as acoustic noise and vibrations, and localized core saturation which tend to reduce reluctance torque. This paper reviews the current state-of-the-art of the MMF harmonic reduction techniques for concentrated winding configurations in PMSMs, including winding split and shift, delta-star connected windings, multiple 3-phase windings, multilayer windings, uneven turn numbers, and stator flux barriers. Their concepts, advantages and disadvantages are presented and assessed.

Keywords: Magnetomotive force(MMF), fractional-slot windings, concentrated windings, permanent-magnet machines.

1 Introduction

Permanent-magnet Synchronous Machines(PMSMs) exhibit high torque density and high energy efficiency over a wide operation range, due to the presence of the permanent magnets[1-2]. Therefore, they have increasingly been employed in a variety of applications, such as industrial drives[3-6], hybrid and electric vehicles[7-12], wind turbine[13-18], aerospace[19-22], marine[23-26], and domestic appliances[27-28], etc.

Subject to the locations of the permanent-magnets, PMSMs can be classified into Surface-mounted Permanent-magnet Machines (SPMs) and Interior Permanent-magnet Machines (IPMs)[29]. With magnets mounted on the rotor surface, SPMs produce torque by the interaction of the magnetic field contributed by permanent-magnets with the armature reaction field produced by the stator magnetic-motive force (MMF). This torque component only depends on the permanent-magnet flux-linkage and *q*-axis current. Therefore, SPMs exhibit a relatively linear torque-current characteristic, good controllability, and low torque ripple. Nevertheless, the surface-mounted magnets result in a large equivalent air-gap because the relative permeability of magnets is close to 1. Hence, the synchronous inductance of the machine is relatively low, leading to a high characteristic current, defined as the ratio of the PM flux to the synchronous inductance, and thereby low field weakening capability[30-31].

* Corresponding Author, E-mail: x.chen.1988@ieee.org.

However, the fractional-slot non-overlapping (concentrated) winding configurations can be utilized to increase the *d*-axis inductance and thus improve the field weakening capability of SPMs[32]. A. M. EL-Refaie et al[33] employed concentrated windings on SPMs and hence developed a 6kW SPM which can deliver constant-power over a 10:1 speed range by increasing the *d*-axis inductance and meeting the optimum field weakening conditions. The authors also investigated the scalability of the concentrated winding configuration for achieving optimal field weakening in SPMs in [34], and showed that the optimal field weakening can be reached over a wide range of machine power ratings from 1kW to 60kW. J. Cros et al[35] performed a synthesis of SPMs with concentrated windings and subsequently compared their performances with those of SPMs using conventional distributed windings. It is shown that by using the concentrated winding configuration, the copper loss can be reduced dramatically owing to both the short end-winding length and the high copper packing factor (if the segmented stator structure is employed). Moreover, the cogging torque can also be significantly reduced when the least common multiple of the slot number and the pole number increases. Therefore, SPMs with concentrated windings exhibit advantages such as high torque density, low copper loss, good field weakening capability, and low cogging torque.

However, by employing concentrated winding configurations in SPMs, the rotor magnets are subjected to a large amount of stator MMF harmonics which are asynchronous with the rotor speed, and

consequently incur high eddy current loss[36]. This can further leads to a high rotor temperature particularly at high speeds, and hence the rotor magnets will suffer from a high risk of irreversible demagnetization.

Compared with SPMs, IPMs have magnets buried in the rotor iron. The IPM rotor topology gives rise to a saliency in reluctances[37]. This difference in the *d*- and *q*-axis reluctances contributes to reluctance torque which is conducive to reduction of PM volume in the IPM[30,38]. To maximize the reluctance torque, the distributed winding configurations are usually employed in IPMs[39]. However, compared to the concentrated windings, the conventional distributed windings have lower copper packing factor (slot fill factor), longer end-winding length, higher cogging torque, and less fault tolerant owing to higher mutual inductance and winding overlapping[40]. Thus, the concentrated winding configurations are of potential to be employed in IPMs, given that the lower and higher order space harmonics in the stator MMF can be suppressed to a desirable level. This can increase IPMs' reluctance torque production, reduce the eddy-current losses in both rotor magnets and rotor iron, and suppress acoustic noise and vibrations.

Therefore, both SPMs and IPMs can greatly benefit from the reduction of the stator MMF harmonics in the concentrated windings. This paper reviews the current state-of-the-art of MMF harmonic reduction techniques. The method for analysis of the MMF harmonics in 3-phase machines will be introduced before various MMF harmonic reduction techniques are introduced and discussed.

2 MMF harmonics

This section describes the method for analyzing the MMF harmonics in any 3-phase concentrated winding with any feasible slot-pole combination.

Assuming *ABC* windings are symmetric and have the same number of turns, the MMF distribution of each phase due to unit current, known as the winding function, can be expressed as Fourier series given in (1).

$$\begin{cases} n_A(\theta_m)=\sum_h\left[N_h\cos\left(h\theta_m+\beta_h\right)\right] \\ n_B(\theta_m)=\sum_h\left[N_h\cos\left(h\theta_m+\beta_h-h\theta_{\text{phm}}\right)\right] \\ n_C(\theta_m)=\sum_h\left[N_h\cos\left(h\theta_m+\beta_h+h\theta_{\text{phm}}\right)\right] \end{cases} \tag{1}$$

where h denotes the harmonic order, N_h is the magnitude of the hth order harmonic, β_h is the phase angle of the hth order harmonic of phase A, θ_{phm} is the mechanical angular displacement between two adjacent phases of a 3-phase winding, and θ_m denotes the space angle at a point of interest in the air-gap with respect to phase A axis as shown in Fig.1.

Due to the symmetrical distribution of a 3-phase winding, θ_{phm}=120° or −120°, depending on the direction of rotation of the MMF working harmonic.

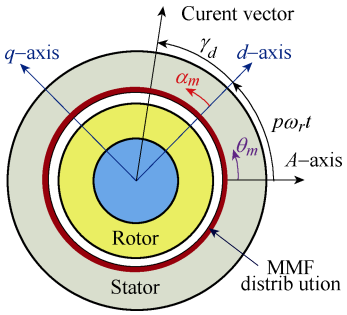

Fig.1 Current vector diagram in *dq*0 and *ABC* coordinate systems[41]

Assuming the current amplitudes in all the phases are identical, the phase currents are expressed by (2).

$$\begin{cases} i_A=I\cos\left(p\omega_r t+\gamma_d\right) \\ i_B=I\cos\left(p\omega_r t+\gamma_d-120°\right) \\ i_C=I\cos\left(p\omega_r t+\gamma_d+120°\right) \end{cases} \tag{2}$$

where I is the current amplitude, p is the pole pair number, ω_r is the rotor angular speed, t is the time, and γ_d is the phase angle between the current vector and the rotor *d*-axis as shown in Fig.1.

The combined MMF of all the 3 phase windings is given in (3).

$$F_s=n_A i_A+n_B i_B+n_C i_C \tag{3}$$

Substituting (1) and (2) into (3), the forward and backward rotating MMF harmonics can be derived and given in (4) and (5) respectively[41].

$$F_f=\frac{1}{2}\sum_h\{N_h I[1+2\cos(h\theta_{\text{phm}}-120°)]\cdot \cos[h\alpha_m+(h-p)\omega_r t-\gamma_d+\beta_h]\} \tag{4}$$

$$F_b=\frac{1}{2}\sum_h\{N_h I[1+2\cos(h\theta_{\text{phm}}+120°)]\cdot \cos[h\alpha_m+(h+p)\omega_r t+\gamma_d+\beta_h]\} \tag{5}$$

where $\alpha_m=\theta_m-\omega_r t$.

For a machine with Q slots and p pole pairs, its periodicity r is subject to the greatest common divider between Q and p, as described in (6).

$$r=\text{GCD}\{Q,p\} \tag{6}$$

The orders of harmonics with non-zero magnitudes for the single phase winding function in (1) are summarized in Table 1, where **Z** denotes the positive integer set. By way of example, in a double layer winding with even Q/r, the orders of harmonics with non-zero magnitudes for the single phase winding function are odd numbers $(2h-1)r$ except for jQ, $j\in\mathbf{Z}$. This is because the even Q/r can form a symmetric pattern with opposite phasors that are π radians out of phase. The harmonics associated with the integer multiples of the slot number, jQ, are cancelled out by the mechanical periodicity. Since 3-phase windings are uniformly displaced in space with respect to each other by 120° electrical degrees all triplen MMF harmonics are eliminated in Q/r slots. This can also be observed in

(4) and (5), where the terms $[1+2\cos(h\theta_{phm}-120°)]$ and $[1+2\cos(h\theta_{phm}+120°)]$ are derived from the 3-phase configuration. Given that jQ is a subset of $3jr$, the orders of MMF harmonics with non-zero magnitudes for a double layer 3-phase winding with an even Q/r are odd numbers $(2h-1)r$ except for $3jr$. The harmonic orders in the other scenarios in Table 1 can also be derived in the same way.

The forward and backward MMF harmonic expressions shown in (4) and (5) can be used to predict any stator MMF harmonic of a conventional 3-phase winding configuration. The magnitude of the hth order winding function harmonic N_h can be obtained by Fast Fourier Transform (FFT) of the winding function waveform of a given winding configuration.

By way of example, for a conventional 3-phase 12-slot 10-pole winding configuration, phase B lags phase A by 8 slots with respect to the rotating direction. Thus, $\theta_{phm}=-120°$. Table 2 lists the values for N_h, $1+2\cos(h\theta_{phm}-120°)$, and $1+2\cos(h\theta_{phm}+120°)$ shown in (4) and (5) to determine the forward and backward MMF harmonics of the 12-slot 10-pole winding configuration up to the 19th order. N_h is normalized against its 5th order working harmonic. The resultant MMF harmonics are calculated using (4) and (5), and plotted in Fig.2 in which 'F' and 'B' denote forward and backward harmonics respectively. Their magnitudes are normalized against that of the 5th order working harmonic. It can be observed that the most detrimental harmonic is the 7th order harmonic, because it not only has a high amplitude but also exhibit a very high frequency seen from the rotor (i.e. 12 times the mechanical frequency).

Table 1 The orders of MMF harmonics with non-zero magnitudes[41]

Winding type	Double layer winding	
Condition	Q/r is even	Q/r is odd
Non-zero harmonic orders for winding function	$(2h-1)r$ except $jQ, j\in\mathbf{Z}$	hr except jQ, $j\in\mathbf{Z}$
Non-zero harmonic orders for 3-phase MMF	$(2h-1)r$ except $3jr, j\in\mathbf{Z}$	hr except $3jr$, $j\in\mathbf{Z}$

Winding type	Single layer winding		
Condition	$Q/(2r)$ is even	$Q/(2r)$ is odd	Q/r is odd & r is even
Non-zero harmonic orders for winding function	$(2h-1)r$ except $jQ, j\in\mathbf{Z}$	hr except $jQ, j\in\mathbf{Z}$	$hr/2$ except $jQ, j\in\mathbf{Z}$
Non-zero harmonic orders for 3-phase MMF	$(2h-1)r$ except $3jr, j\in\mathbf{Z}$	hr except $3jr, j\in\mathbf{Z}$	$hr/2$ except $3jr/2, j\in\mathbf{Z}$

Table 2 MMF harmonic expression breakdown of a conventional 3-phase 12-slot 10-pole winding configuration

Harmonic order	N_h	$1+2\cos(h\theta_{phm}-120°)$	$1+2\cos(h\theta_{phm}+120°)$
1	0.36	0	3
3	0.89	0	0
5	1.00	3	0
7	0.72	0	3
9	0.30	0	0
11	0.03	3	0
13	0.03	0	3
15	0.18	0	0
17	0.29	3	0
19	0.26	0	3

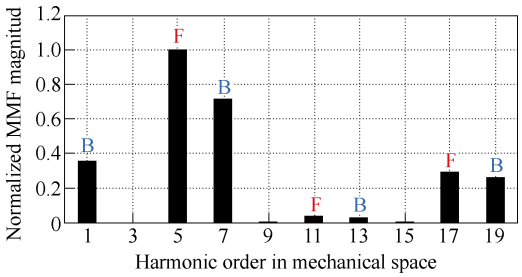

Fig.2 MMF spectrum of the conventional 3-phase 12-slot 10-pole winding configuration

The foregoing technique can be used to analyze MMF harmonic distributions of all 3-phase and multiple 3-phase windings, including most of the winding configurations designed to reduce MMF harmonics that will be described and discussed in the subsequent sections.

3 MMF harmonic reduction techniques

In an ideal 3-phase machine, only MMF working harmonic should be present and all other harmonics eliminated. In this section, the techniques to reduce undesirable MMF harmonics reported in literature are outlined, including winding split and shift, delta-star connected windings, multiple 3-phase windings, multilayer windings, uneven turn numbers, and stator flux barriers. The other techniques which are of obvious disadvantage have not been discussed in this paper, such as uneven tooth width and uneven back-iron.

3.1 Winding split and shift

G. Dajaku and D. Gerling[42-43] proposed a 24-slot 10-pole winding configuration, as shown in Fig.3, to minimize the 1st and 7th order MMF harmonics of the conventional 12-slot 10-pole winding configuration. The MMF spectrum of the conventional 12-slot 10-pole winding configuration is shown in Fig.2. The concept is to divide the original 12-slot 10-pole windings into 2 sets, arrange them with a specific mechanical phase shift, and connect them in series, as illustrated in Fig.3. The mechanical phase shift, α_w, between these 2 sets of windings is determined by the order of MMF harmonic to be eliminated. Mathematically, this concept is to reshape the single phase winding function to make the magnitude of the hth order harmonic of the winding function, N_h in (1), to be zero.

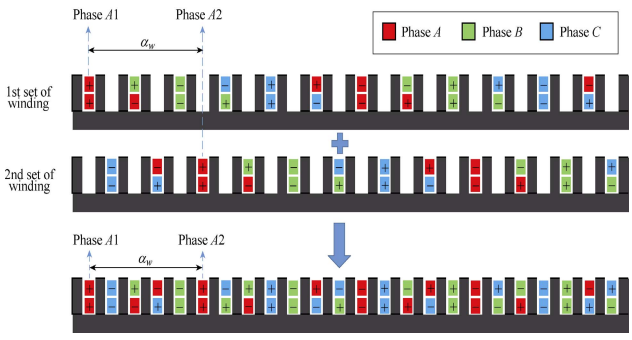

Fig.3 Schematic of the 24-slot 10-pole winding configuration proposed in [42-43]

To eliminate the 7th order MMF harmonic shown in Fig.2, the optimal mechanical phase shift α_w is selected to be slightly higher than 2.5 times the tooth pitch angle. Thus, uneven tooth width technique has to be utilized. Although with this technique the 7th order MMF harmonic has been significantly reduced, the reduction in the 1st order MMF harmonic is only 20% approximately. Therefore, to attenuate the 1st order MMF harmonic, uneven turn numbers for the neighboring phase coils are also employed. Fig.4 illustrates the MMF spectrum of the proposed 24-slot 10-pole winding configuration with winding split and shift, uneven tooth widths, and also uneven turn numbers techniques. A significant reduction in the 1st and 7th order MMF harmonics can be observed. In doing so, however, the winding factor of the fundamental is slightly reduced compared with the conventional 12-slot, 10-pole winding configuration.

V. I. Patel and J. Wang et al[44-45] proposed a 6-phase 18-slot 10-pole winding configuration whose schematic can be found in Fig.5. The concept is to split the 3-phase 9-slot 8-pole windings into two sets and apply appropriate phase shift for the specific harmonic cancellation. To enhance the machine fault-tolerant capability, 6-phase (two 3-phase) technique is employed and these two 3-phase windings are fed by two separated inverters. The mechanical phase shift between these two sets of 3-phase windings is selected to eliminate the most MMF harmonics. The currents fed into these two sets of 3-phase windings have no phase shift in time domain.

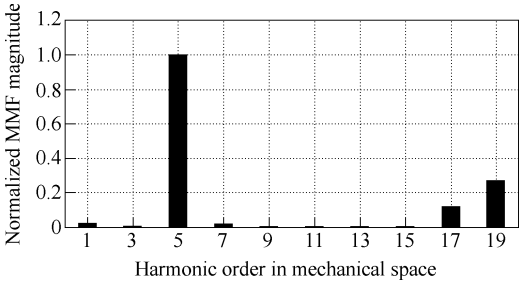

Fig.4 MMF spectrum of the proposed 24-slot 10-pole winding configuration (with uneven turn numbers) in [42-43]

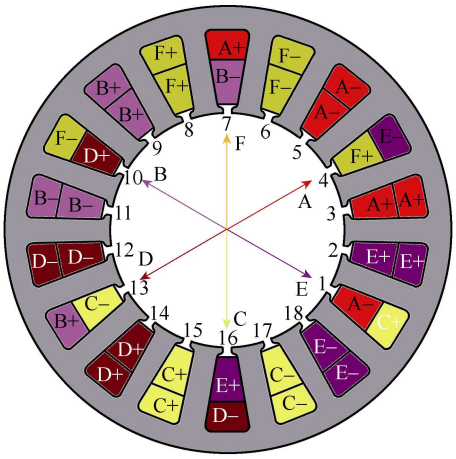

Fig.5 Schematic of the 6-phase 18-slot 8-pole winding configuration proposed in [44-45]

Fig.6 compares the MMF spectra of the 6-phase 18-slot 8-pole winding configuration with those of the conventional 9-slot 8-pole windings whose MMF spectrum can be calculated using (4) and (5). It can be seen that 1st, 5th, 7th, 11th, 13th, 17th, 19th, 23rd … orders of MMF harmonics are completed eliminated.

J. Wang et al [46] also devised all the feasible slot-pole combinations with the foregoing technique. The optimal phase shift between these two 3-phase windings for various slot-pole combinations are given.

P. B. Reddy et al[47] derived a generic approach to the selection of the optimal mechanical phase shift of the two sets of windings after splitting the phase windings. Uneven tooth width design is considered to reach the best harmonic cancellation effects.

A. S. Abdel-Khalik et al[48] developed a 6-phase 24-slot 10-pole winding configuration whose schematic is shown in Fig.7. The concept is also to split phase windings into two 3-phase sets. The phase shifts in both space and time between the two 3-phase phase sets are selected to eliminate the most undesirable MMF harmonics. Fig.8 compares the MMF spectra of the 6-phase 24-slot 10-pole winding configuration with those of the 3-phase 24-slot 10-pole windings. It can be seen that with the introduced phase shift between the two 3-phase sets in time domain, the 1st order MMF harmonic which is present in the 3-phase machines has been cancelled out.

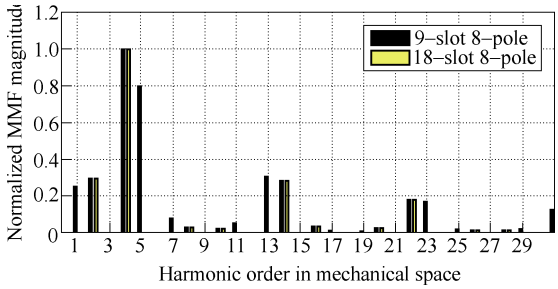

Fig.6 MMF spectra comparison between the conventional 9-slot 8-pole and the 6-phase 18-slot 8-pole winding configuration proposed in [44-45]

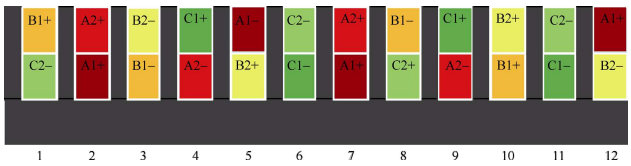

Fig.7 Schematic of the 6-phase 24-slot 10-pole winding configuration (12 slots displayed) proposed in [48]

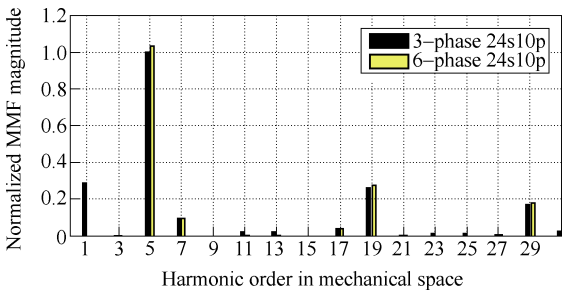

Fig.8 MMF spectra comparison of the 3-phase and 6-phase 24-slot 10-pole winding configurations proposed in [48]

All of the foregoing techniques can reduce or eliminate certain MMF harmonics, particularly the most detrimental harmonic whose order is close to the working harmonic. However, by splitting the phase windings into two 3-phase sets, slot and coil numbers are doubled. In order to maintain a decent fundamental winding factor, a coil span of 2 slots is employed. Thus, these proposed windings are no longer concentrated or tooth-wound windings in conventional sense, thereby compromising the advantages of the concentrated windings.

3.2 Delta-star windings

G. Dajaku and D. Gerling et al[49-50] proposed an 18-slot 10-pole concentrated winding configuration with a delta-star connection. The idea is to create two sets of windings, one in star connection and other in delta connection. By exploiting the phase shift between the MMFs produced by the two sets of windings some undesirable harmonics can be eliminated with appropriate selection of the number of coils in each winding set. Meanwhile, the number of slots is increased by $k_n \cdot m$ where k_n is the number of winding sets and m is the number of phases. By way of example, Fig.9 (a) shows the coil distribution and connection of phase A winding in the conventional 12-slot 10-pole machine. By expanding 12 slots to 18 slots, phase A now has 6 coils which are grouped into $A1$ and $A2$ as shown in. Fig.9(b). Thus, this winding arrangement maintains the concentrated winding configuration in which the coil span equals 1 slot pitch. However, for the same pole pairs, the coil span in electrical degree is much reduced. This greatly penalizes the fundamental winding factor and thus the torque production capability is compromised.

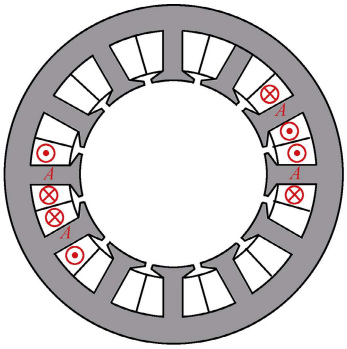

(a) Conventional 12-slot 10-pole windings with phase A

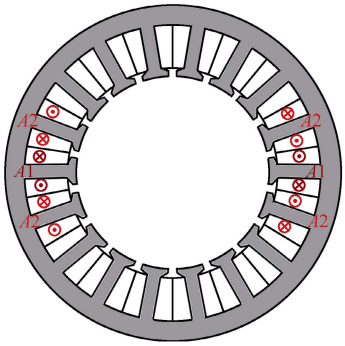

(b) New 18-slot 10-pole windings with two sets of phase A

Fig.9 Concept explanation of the 18-slot 10-pole windings proposed in [49-50]

These two sets of windings shown in Fig.9(b) are connected using delta-star combinations to produce the phase shift in the currents flowing in them. Fig.10 illustrates the schematics of the developed 18-slot 10-pole winding and its delta-star connection diagram. The delta and star windings in each phase have 4 and 2 coils respectively. The electrical phase shift between the delta and star connected windings is 30°, while the current magnitude in the star connected windings are $\sqrt{3}$ times those in the delta connected windings. Thus, the number of turns per phase of the delta windings needs $\sqrt{3}$ times greater than those in the star windings to balance the MMF magnitudes of the two sets of windings and cancel out the unwanted MMF harmonics.

Fig.11 compares the MMF spectra of the 18-slot 10-pole winding configuration with those of the conventional 12-slot 10-pole windings. It can be seen that the 1st, 7th, 11th, 13th, 17th, 19th ⋯ orders of MMF harmonics have been eliminated whereas the 13th order harmonic increases.

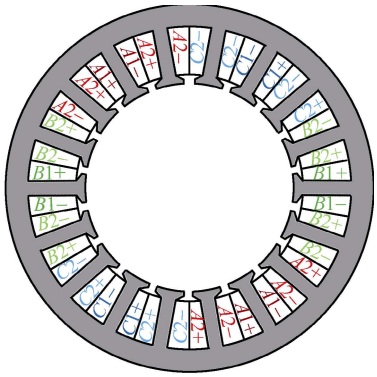

(a) Winding schematic

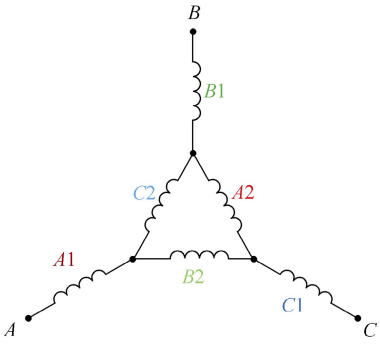

(b) Delta-star connection

Fig.10 Schematics of the 18-slot 10-pole winding configuration with delta-star connections proposed in [49-50]

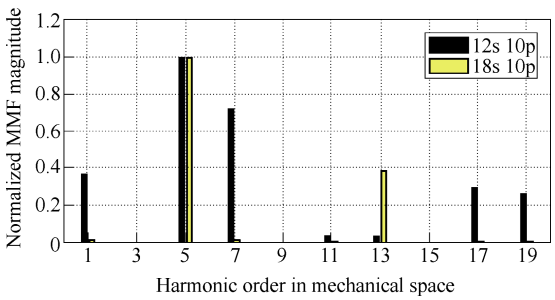

Fig.11 MMF spectra comparison between the conventional 12-slot 10-pole and the 18-slot 10-pole winding configuration proposed in [49-50]

A. S. Abdel-Khalik et al[51] proposed a generic dual n-phase winding configuration with delta-star connections for n-phase PM machine occupying $4n$ slots, to cancel out all the sub-harmonics of the winding MMF. Compared to the techniques proposed in [49-50], the slot and coil numbers are not increased. Instead, the original coils are split into 2 sets of windings which are arranged with a specific phase shift in space. Thus, the fundamental winding factor is not penalized. The delta-star connection is employed to generate a phase shift in time domain for the cancellation of some undesirable MMF harmonics.

The winding configuration are applied in [51] to a 3-phase 12-slot 10-pole winding configuration with delta-star connection and to a 5-phase 20-slot 18-pole winding configuration with pentagon-star connection, as shown in Fig.12 and Fig.13, respectively.

Fig.14 shows the MMF spectra of the 3-phase 12-slot 10-pole and 5-phase 20-slot 18-pole windings proposed in [51]. It can be observed that the sub-harmonics and some of the higher order MMF harmonics have been eliminated while the working harmonic and some higher order harmonics are increased due to slightly higher winding distribution factors.

However, the MMF harmonic reduction by this winding technique is limited because the electrical phase shift between the delta and star windings is restricted to 30° and that between the pentagon and star windings to 18°. Consequently the most detrimental harmonic whose order is close to the working harmonic is not affected.

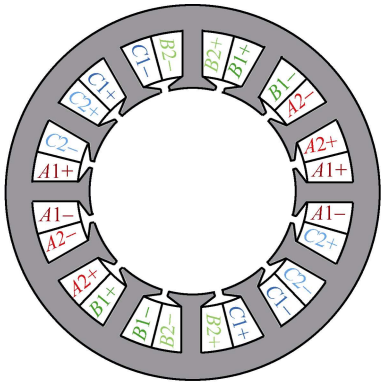

(a) 3-phase 12-slot 10-pole windings

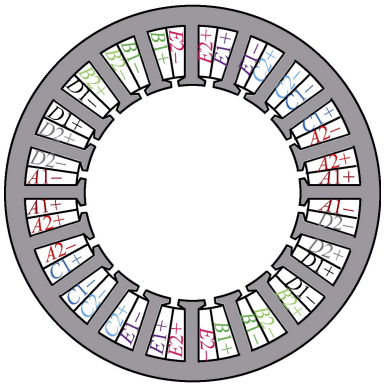

(b) 5-phase 20-slot 18-pole windings

Fig.12 Schematics of the winding configurations proposed in [51]

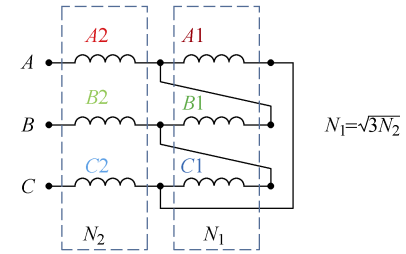

(a) 3-phase 12-slot 10-pole windings

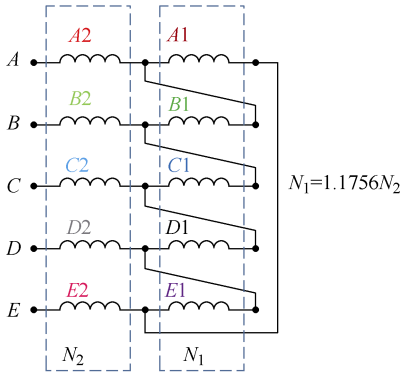

(b) 5-phase 20-slot 18-pole windings

Fig.13 Connections of the winding configurations proposed in [51]

Note: N_1 and N_2 denotes the number of turns associated with the delta- or pentagon- connected and the star-connected windings, respectively.

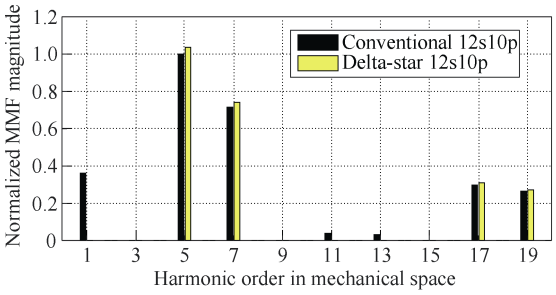

(a) 3-phase 12-slot 10-pole windings

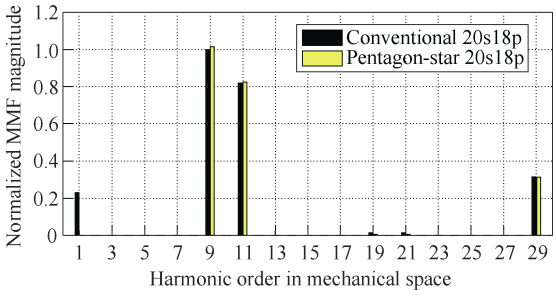

(b) 5-phase 20-slot 18-pole windings

Fig.14 MMF spectra of the winding configurations proposed in [51]

3.3 Multiple 3-phase windings

X. Chen and J. Wang et al[41, 52] proposed a generic approach to reduction of MMF harmonics using multiple 3-phase winding configurations, and subsequently devised a 9-phase 18-slot 14-pole machine. Fig.15 shows the MMF harmonic cancellation principle using multiple 3-phase winding configurations. The three 3-phase windings are uniformly arranged in space but with a specific spatial phase angle with respect to each other, as shown in Fig.15(a). The phase shift in time for

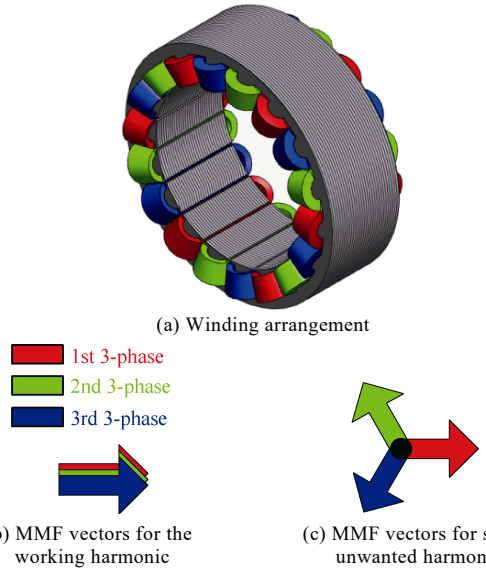

(a) Winding arrangement

(b) MMF vectors for the working harmonic

(c) MMF vectors for some unwanted harmonics

Fig.15 Illustration of MMF harmonic cancellation principle using multiple 3-phase winding configurations proposed in [41, 52]

the currents in each 3-phase set can also be selected in order to eliminate unwanted harmonics. The condition to cancel out a given order MMF harmonic is to select appropriate space and time phase shifts so that the MMF vectors produced by the three 3-phase windings form a balanced 3-phase system, as illustrated in Fig.15(c), while their working harmonic vectors overlap with each other, as shown in Fig.15(b). Indeed, this multiple 3-phase winding configuration introduces an additional 'degree of freedom' in the MMF harmonic cancellation mechanism.

The generic mathematic expressions for the forward and backward MMF harmonics in a multiple 3-phase windings have been derived based on (4) and (5), and they are given in (7) and (8), respectively.

$$F_f = \frac{1}{2}\sum_h \{N_h I[1+2\cos(h\theta_{\text{phm}} - 120°)]\cdot \sum_k \cos[h\alpha_m + (h-p)\omega_r t - \gamma_d + \beta_{kh} + (k-1)\theta_\Delta]\} \quad (7)$$

$$F_b = \frac{1}{2}\sum_h \{N_h I[1+2\cos(h\theta_{\text{phm}} + 120°)]\cdot \sum_k \cos[h\alpha_m + (h+p)\omega_r t + \gamma_d + \beta_{kh} - (k-1)\theta_\Delta]\} \quad (8)$$

where k denotes the kth 3-phase set, β_{kh} is the phase angle of the hth order spatial harmonic of the kth set 3-phase winding, and θ_Δ is the phase shift angle of the currents between the (k+1)th and kth 3-phase sets.

The condition to eliminate the hth order MMF harmonic is that the combined phase shift angles between the kth and (k+1)th 3-phase sets denoted as θ_{fw} and θ_{bw} for the forward and backward MMF harmonics satisfy (9) and (10), respectively.

$$\theta_{fw} = \beta_{(k+1)h} - \beta_{kh} + \theta_\Delta = \pm 360°/K + q_f 360° \quad q_f \in Z \quad (9)$$

$$\theta_{bw} = \beta_{(k+1)h} - \beta_{kh} - \theta_\Delta = \pm 360°/K + q_b 360° \quad q_b \in Z \quad (10)$$

where K is the number of 3-phase sets. The above conditions lead to the second summation in (7) and (8) becoming zero and hence the hth order harmonic is eliminated.

Based on the foregoing approach, a 9-phase 18-slot 14-pole winding configuration for IPM machines is developed and its schematic is illustrated in Fig.16. The MMF spectra comparison of the conventional 3-phase and 9-phase 18-slot 14-pole winding configurations is shown in Fig.17. The MMF spectrum of the conventional 3-phase winding is calculated using (4) and (5). It can be seen that by employing the multiple 3-phase winding configuration, the 1st, 5th, 13th, 17th, 19th, 23rd ⋯ order harmonics are cancelled out while the 7th (working harmonic for 14-pole), 11th, 25th, 29th ⋯ order harmonics slightly increase due to higher winding distribution factors.

This technique also contributes to a degree of fault tolerance in that the machine can continue to operate even if one 3-phase windings/drive fails.

The use of multiple 3-phase winding configurations and inverters may not be a disadvantage as the reduction of current rating in each 3-phase system would facilitate inverter heat dissipation and integration into machine housing, particularly for high power drives.

3.4 Multilayer windings

M. V. Cistelecan et al[53-54] proposed concentrated multilayer winding configurations whose schematics are illustrated in Fig.18. Two conventional windings, 12-slot 10-pole and 9-slot 8-pole, are chosen to demonstrate the MMF harmonic cancellation effects with the multilayer winding techniques. The concept is to split the coils into two sets and shift one set of coils

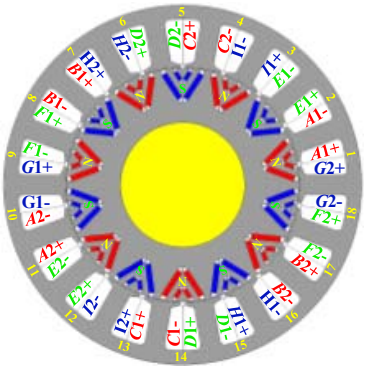

Fig.16 Schematic of the 9-phase 18-slot 14-pole winding configuration proposed in [41, 52]

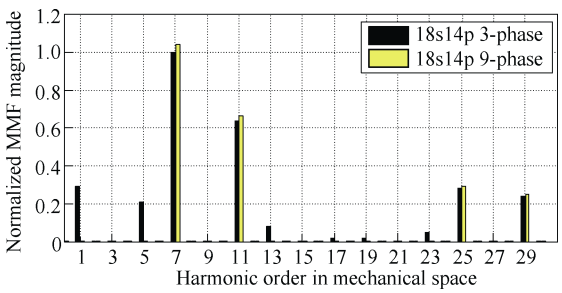

Fig.17 MMF spectra comparison of the conventional 3-phase and 9-phase 18-slot 14-pole winding configurations proposed in [41, 52]

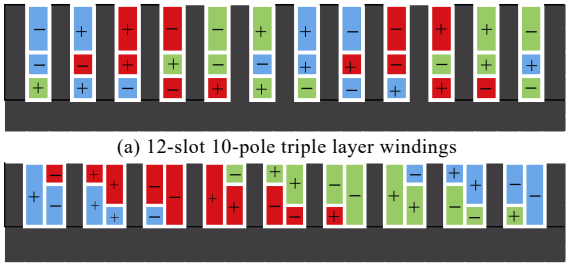

(a) 12-slot 10-pole triple layer windings

(b) 9-slot 8-pole quadruple layer windings

Fig.18 Schematics of the multilayer winding configurations proposed in [53-54]

by one or more slots, while maintaining the same number of slot for a given number of pole pairs. Initially four layers of windings are devised. By merging the coils which are in the same slot and also in the same phase, a triple layer winding configuration, as shown in Fig.18(a) can be developed. If there are no coils to satisfy both conditions, the quadruple layer winding configuration, as shown in Fig.18(b), will be employed. The number of turns per coil can be adjusted to reduce the most MMF harmonics. By way of example, the number of turns per coil of the top layer (adjacent to the back-iron) windings in Fig.18(a) is designed to be √3 times of those of the other layers.

Fig.19(a) and (b) compare the MMF spectra of the developed triple layer 12-slot 10-pole and quadruple 9-slot 8-pole windings with those of their double layer counterparts whose MMF spectra can be calculated using (4) and (5). It shows that the sub-harmonics and some higher order harmonics can be eliminated or greatly diminished.

A. S. Abdel-Khalik et al[55] proposed a triple layer 12-slot 10-pole winding configuration with the delta-star connection as shown in Fig.20(d), and thereafter performs a comparative study with the other three 12-slot 10-pole winding types including the conventional double layer winding denoted as 'winding 1' in

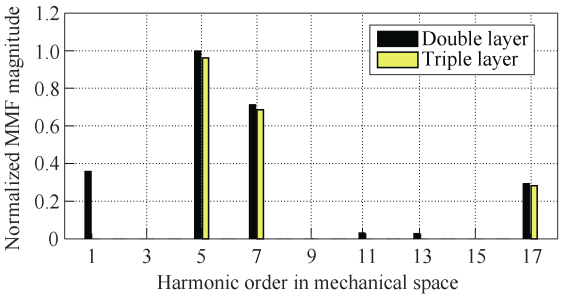

(a) 12-slot 10-pole double and triple layer windings

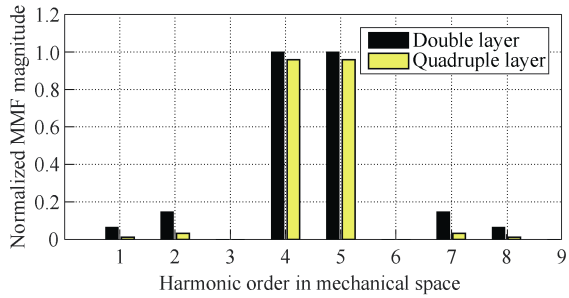

(b) 9-slot 8-pole double and quadruple layer windings

Fig.19 MMF spectra comparisons of the multilayer winding configurations proposed in [53, 54]

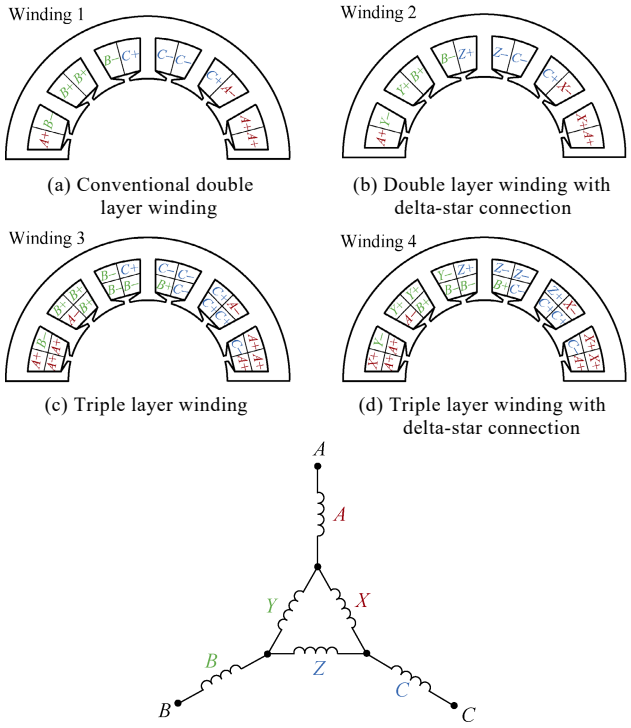

(a) Conventional double layer winding

(b) Double layer winding with delta-star connection

(c) Triple layer winding

(d) Triple layer winding with delta-star connection

(e) Delta-star connection

Fig.20 Schematics of 12-slot 10-pole winding configurations proposed in [55]

Fig.20(a), double layer winding with delta-star connection denoted as 'winding 2' in Fig.20(b), and triple layer winding denoted as 'winding 3' in Fig.20(c).

Fig.21 compares the MMF spectra of these four types of 12-slot 10-pole winding configurations. The MMF spectrum of 'winding 1' can be calculated using (4) and (5). It can be observed that both the double layer winding with delta-star connection and the proposed triple layer winding with delta-star connection have the best MMF harmonic cancellation effects, eliminating the sub-harmonics and some of higher order harmonics. However, the proposed triple layer winding with delta-star connection compromises the fundamental winding factor and thus slightly penalizes the torque production, although it may maintain the benefits of multilayer designs, such as higher saliency ratio and reluctance torque component.

The foregoing multilayer winding configurations increases the complexity of connection and results in lower fundamental winding factor and hence low torque capability. In addition, the most detrimental harmonic whose order is close to that of the working harmonic is not significantly reduced.

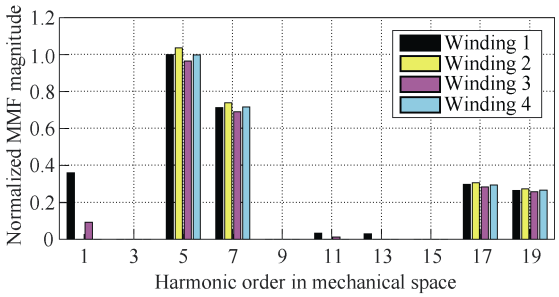

Fig.21 MMF spectra comparison of the multilayer winding configurations proposed in [55]

3.5 Uneven turn numbers

G. Dajaku and D. Gerling[56-57] developed a 12-slot 10-pole winding configuration with uneven number of turns in the neighboring slots, as illustrated in Fig.22. The mathematic relation between $n1$ and $n2$ shown in Fig.22 is determined by the order of MMF harmonic to be suppressed. To easily realize uneven turn numbers, $n1$ and $n2$ differ by 1. Thus, the slot with less turn number should not complete the last turn, as illustrated in Fig.22. The ratio of $n1$ to $n2$ determines the MMF harmonic cancellation effect. By way of example, the 1st order MMF harmonic can be eliminated when the ratio of $n1$ to $n2$ equals 0.87. Therefore, in this application, $n1$ and $n2$ are designed to be 7 and 8 respectively. Thus, the 1st order MMF harmonic is reduced by 97.5% with the ratio of $n1$ to $n2$ equaling 0.875. It can also be inferred that the MMF harmonic cancellation effects are negligible when the number of turns per coil relatively high because the ratio of $n1$ to $n2$ will be close to be 1 if $n1$ and $n2$ only differ by 1.

Fig.23 compares the MMF spectra of the conventional 12-slot 10-pole winding configuration and that with uneven number of turns proposed in [56-57]. It can be seen that the 1st, 11th, 13th order MMF harmonics has been greatly diminished. However, the most detrimental 7th MMF harmonic is not reduced.

The foregoing technique restricts the difference in the uneven turn numbers to be only 1 turn. Therefore, the ability to reduce MMF harmonics by this technique is quite limited when the turn number has to be designed high. On the other hand, it is not practical to have the difference in the number of turns on two sides of a coil being greater than 1. Further, uneven Ampere turn distribution in slots lead to less effective utilization of the slot areas and localized saturation in the stator teeth, compromising the electromagnetic performances.

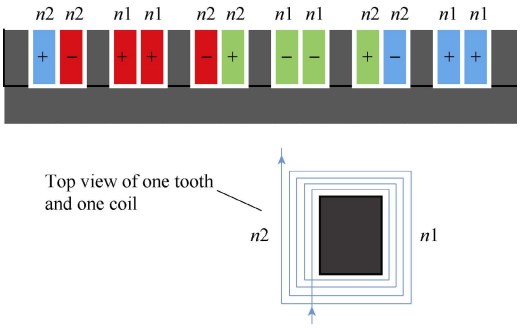

Fig.22 Schematic of the winding configuration with uneven number of turns proposed in [56-57]

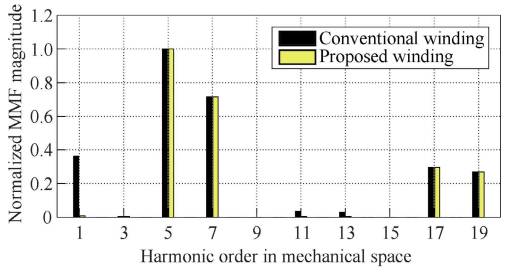

Fig.23 MMF spectra comparison of the conventional 12-slot 10-pole winding configuration and that with uneven number of turns proposed in [56-57]

3.6 Stator flux barriers

G. Dajaku et al [58] proposed a new 12-slot 10-pole machine topology with flux barriers located at the stator back-iron. The introduced flux barriers significantly increase the reluctance to the 1st order MMF harmonic while the reluctance to other higher order harmonics are less affected. Consequently, the air-gap flux density due to the 1st MMF harmonic is reduced.

The proposed single and double layer 12-slot 10-pole machines with stator flux barriers are illustrated in Fig.24 (a) and (b) respectively. The sizes of these flux barriers can be optimized to obtain the best harmonic cancellation effect.

Fig.25 compares the air-gap flux density spectra of the conventional 12-slot 10-pole winding configuration and that with stator flux barriers proposed in [58] under excitations of the stator currents only. It shows that the 1st, 11th and 13th harmonics of air-gap flux density of the single layer windings are reduced by approximately 50%. However, these air-gap flux density harmonics of the double layer windings are eliminated, whereas the 5th working harmonic is slightly penalized.

While the concept is simple to be implemented there a number of disadvantages associated with this technique. First the harmonic cancellation effects may be compromised at heavy load condition since the saturation in the stator core affects the reluctance in the magnetic circuit. The fundamental winding factor and

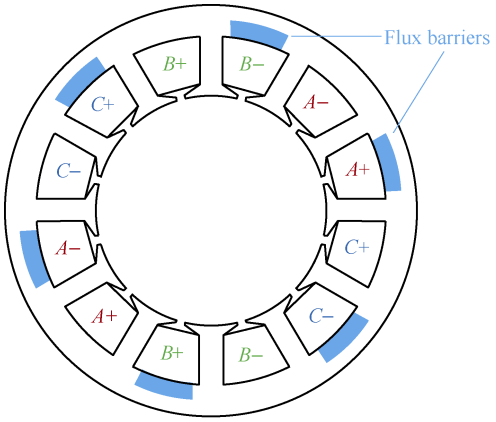

(a) Single layer windings

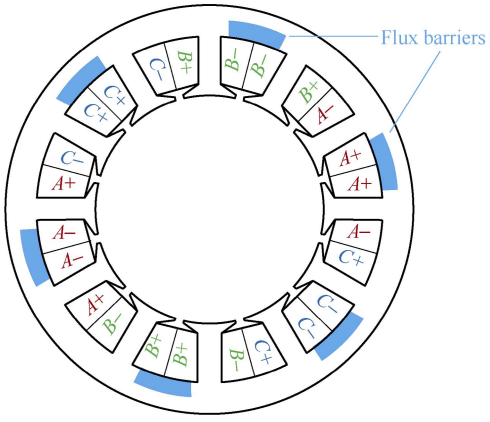

(b) Double layer windings

Fig.24 Schematics of 12-slot 10-pole machines with stator flux barriers proposed in [58]

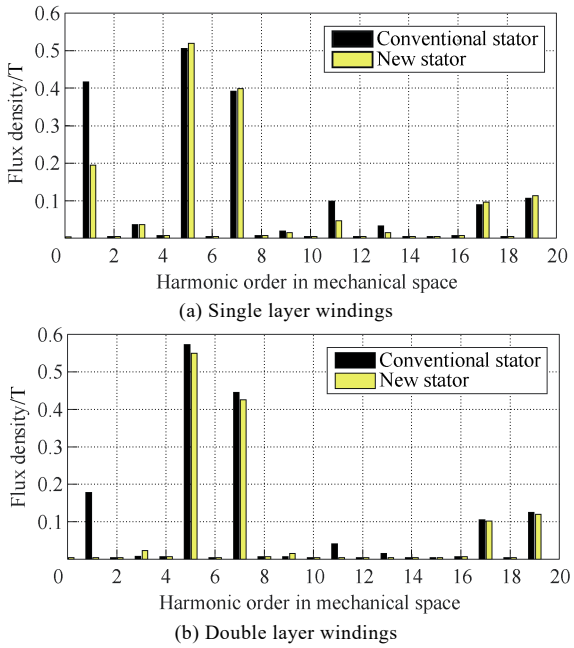

Fig.25 Air-gap flux density spectra comparison of the conventional 12-slot 10-pole winding configuration and that with stator flux barriers proposed in [58]

torque production may be compromised without careful design. In addition the flux linkages generated by permanent-magnets are slightly reduced due to higher reluctances caused by the flux barriers in the stator, and thus the magnetic loading is reduced with the same amount of permanent-magnets.

4 Conclusion

This paper reviews the current state-of-the-art of the MMF harmonic reduction techniques for concentrated winding configurations in PMSMs, including winding split and phase shift, delta-star windings, multiple 3-phase windings, multilayer windings, uneven turn numbers, and stator flux barriers. Their concepts, advantages and disadvantages have been assessed and discussed.

The technique of employing winding split and phase shift can eliminate the most detrimental MMF harmonic whose order is close to that of the working harmonic. However, to maintain a decent fundamental winding factor, a coil span of 2 slots has to be employed. Therefore, the neighboring coils overlap with each other, and thus this technique no longer possess some advantages of the conventional concentrated windings.

The other techniques maintain the concentrated winding configurations, yet cannot significantly reduce the most detrimental MMF harmonic whose order is close to that of the working harmonic, without compromising the fundamental winding factor and torque capability. The delta-star winding configuration can only produce a specific phase shift between the delta and star connected winding sets. The multiple 3-phase winding configuration requires the use of the multiple 3-phase inverters. The multilayer winding configuration increases the complexity of connection and also results in lower fundamental winding factor and hence low torque capability. The winding configuration with uneven number of turns has limited MMF harmonic cancellation effects and results in the uneven Ampere turn distribution in slots. This also leads to less effective utilization of the slot areas and cause localized saturation in the stator teeth, compromising the electromagnetic performances. The stator flux barrier technique requires more delicate balance between the electrical and magnetic loadings in the stator design, and may compromise the torque production capability while its harmonic cancellation effects at heavy load condition is limited.

Selection of the most appropriate technique is application dependent. For example, in high power drives, use of multiple 3-phase windings would reduce inverter rating for each 3-phase set and facilitates heat spreading and dissipation. Thus, the technique with multiple 3-phase winding configuration can be readily exploited without increase in cost.

References

[1] M. W. Brainard, "Synchronous machines with rotating permanent-magnet fields; part i. characteristics and mechanical construction [includes discussion]," *Transactions of the American Institute of Electrical Engineers. Part III: Power Apparatus and Systems,* vol. 71, no. 1, p. 1, 1952.

[2] K. T. Chau, C. C. Chan, and C. Liu, "Overview of permanent-magnet brushless drives for electric and hybrid electric vehicles," *IEEE Transactions on Industrial Electronics,* vol. 55, no. 6, pp. 2246-2257, 2008.

[3] Q. Chen, G. Liu, W. Zhao, L. Qu, and G. Xu, "Asymmetrical SVPWM fault-tolerant control of five-phase PM brushless motors," *IEEE Transactions on Energy Conversion,* vol. 32,no. 1, pp. 12-22, 2017.

[4] J. Liu, T. Matsuo, T. A. Nondahl, P. B. Schmidt, T. M. Rowan, and R. J. D. Lange, "Implementation and performance of position sensorless PMSM control in industrial drives," in *IEEE Industry Application Society Annual Meeting*, pp. 1-8, 2014.

[5] Y. Wu, H. Li, M. Y. Q. Li, and Y. Bi, "The design of industrial sewing machine servo system based on PMSM," in *IEEE International Conference on Mechatronics and Automation*, pp. 98-103,2012.

[6] W. Wang, M. Cheng, B. Zhang, Y. Zhu, and S. Ding, "A fault-tolerant permanent-magnet traction module for subway applications," *IEEE Transactions on Power Electronics,* vol. 29, no. 4, pp. 1646-1658, 2014.

[7] I. Boldea, L. N. Tutelea, L. Parsa, and D. Dorrell, "Automotive electric propulsion systems with reduced or no permanent magnets: an overview," *IEEE Transactions on Industrial Electronics,* vol. 61, no. 10, pp. 5696-5711, 2014.

[8] D. Dorrell, L. Parsa, and I. Boldea, "Automotive electric motors, generators, and actuator drive systems with reduced or no permanent magnets and innovative design concepts," *IEEE Transactions on Industrial Electronics,* vol. 61, no. 10, pp. 5693-5695, 2014.

[9] J. Wang, X. Yuan, and K. Atallah, "Design optimization of a surface-mounted permanent-magnet motor with concentrated windings for electric vehicle applications," *IEEE Transactions on Vehicular Technology,* vol. 62, no. 3, pp. 1053-1064, 2013.

[10] A. Wang, Y. Jia, and W. L. Soong, "Comparison of five topologies for an interior permanent-magnet machine for a hybrid electric vehicle," *IEEE Transactions on Magnetics,* vol. 47, no. 10, pp. 3606-3609, 2011.

[11] X. Chen, J. Wang, P. Lazari, and L. Chen, "Permanent magnet assisted synchronous reluctance machine with fractional-slot winding configurations," in *2013 International Electric Machines & Drives Conference*, pp. 374-381, 2013.

[12] J. Li, Y. Xu, J. Zou, Q. Wang, and W. Liang, "Analysis and reduction of magnet loss by deepening magnets in interior permanent-magnet machines with a pole/slot ratio of 2/3," *IEEE Transactions on Magnetics,* vol. 51, no. 11, pp. 1-4, 2015.

[13] L. Jian, K. T. Chau, and J. Z. Jiang, "A magnetic-geared outer-rotor permanent-magnet brushless machine for wind power generation," *IEEE Transactions on Industry Applications,* vol. 45, no. 3, pp. 954-962, 2009.
[14] Z. Xiang-Jun, Y. Yongbing, Z. Hongtao, L. Ying, F. Luguang, and Y. Xu, "Modelling and control of a multi-phase permanent magnet synchronous generator and efficient hybrid 3L-converters for large direct-drive wind turbines," *IET Electric Power Applications,* vol. 6, no. 6, pp. 322-331, 2012.
[15] R. S. Semken, M. Polikarpova, P. Roytta, J. Alexandrova, J. Pyrhonen, and J. Nerg, "Direct-drive permanent magnet generators for high-power wind turbines: benefits and limiting factors," *IET Renewable Power Generation,* vol. 6, no. 1, pp. 1-8, 2012.
[16] R. S. Semken, C. Nutakor, A. Mikkola, and Y. Alexandrova, "Lightweight stator structure for a large diameter direct-drive permanent magnet synchronous generator intended for wind turbines," *IET Renewable Power Generation,* vol. 9, no. 7,pp. 711-719, 2015.
[17] E. Prieto-Araujo, A. Junyent-Ferré, D. Lavènia-Ferrer, and O. Gomis-Bellmunt, "Decentralized control of a nine-phase permanent magnet generator for offshore wind turbines," *IEEE Transactions on Energy Conversion,* vol. 30, no. 3, pp. 1103-1112, 2015.
[18] A. Penzkofer, and K. Atallah, "Analytical modeling and optimization of pseudo-direct drive permanent magnet machines for large wind turbines," *IEEE Transactions on Magnetics,* vol. 51, no. 12, pp. 1-14, 2015.
[19] W. Xueqing, Z. Wang, J. Chen, M. Cheng, and X. Liang, "Direct torque control of dual three-phase PMSM drives based on two-step voltage vector synthesis SVM," in *2016 IEEE 8th International Power Electronics and Motion Control Conference (IPEMC-ECCE Asia)*, pp. 641-647, 2016.
[20] H. Guo, J. Xu, and Y. H. Chen, "Robust control of fault-tolerant permanent-magnet synchronous motor for aerospace application with guaranteed fault switch process," *IEEE Transactions on Industrial Electronics,* vol. 62, no. 12, pp. 7309-7321, 2015.
[21] X. Jiang, W. Huang, R. Cao, Z. Hao, and W. Jiang, "Electric drive system of dual-winding fault-tolerant permanent-magnet motor for aerospace applications," *IEEE Transactions on Industrial Electronics,* vol. 62, no. 12,pp. 7322-7330, 2015.
[22] A. G. Sarigiannidis, M. E. Beniakar, P. E. Kakosimos, A. G. Kladas, L. Papini, and C. Gerada, "Fault tolerant design of fractional slot winding permanent magnet aerospace actuator," *IEEE Transactions on Transportation Electrification,* vol. 2, no. 3, pp. 380-390, 2016.
[23] K. Yuen, K. Thomas, M. Grabbe, P. Deglaire, M. Bouquerel, D. Osterberg, "Matching a permanent magnet synchronous generator to a fixed pitch vertical axis turbine for marine current energy conversion," *IEEE Journal of Oceanic Engineering,* vol. 34, no. 1, pp. 24-31, 2009.
[24] L. Yang, L. Fei, Y. Jinjun, L. Jiansheng, and G. Yuting, "Optimal design of a Halbach magnetized permanent magnet motor applied in electrical marine propulsion system," in *2014 IEEE Conference and Expo Transportation Electrification Asia-Pacific (ITEC Asia-Pacific)*, pp. 1-5, 2014.
[25] G. Jining, Y. Enxiang, and Z. Aihua, "Vector control system of permanent magnet synchronous motor for marine electric propulsion," in *2014 International Conference on Mechatronics and Control (ICMC)*, 2014, pp. 2126-2129.
[26] K. Ahsanullah, S. K. Panda, R. Shanmukha, and S. Nadarajan, "Inter-turns fault diagnosis for surface permanent magnet based marine propulsion motors," in *2016 IEEE 2nd Annual Southern Power Electronics Conference (SPEC)*, 2016, pp. 1-6.
[27] A. C. Smith, and A. K. B. Wong, "Performance of line-start single phase permanent magnet motors for domestic applications," in *Thirty-First IAS Annual Meeting on Industry Applications(IAS '96),* vol.1, pp. 503-510, 1996.
[28] E. Sulaiman, G. M. Romalan, and N. A. Halim, "Skewing and notching configurations for torque pulsation minimization in spoke-type interior permanent magnet motors," in *International Conference on Control, Electronics, Renewable Energy and Communications (ICCEREC)*, pp. 202-207, 2016.
[29] P. B. Reddy, A. M. El-Refaie, K. K. Huh, J. K. Tangudu, and T. M. Jahns, "Comparison of interior and surface PM machines equipped with fractional-slot concentrated windings for hybrid traction applications," *IEEE Transactions on Energy Conversion,* vol. 27, no. 3, pp. 593-602, 2012.
[30] A. Vagati, G. Pellegrino, and P. Guglielmi, "Comparison between SPM and IPM motor drives for EV application," in *The XIX International Conference on Electrical Machines - ICEM 2010*, pp. 1-6,2010.
[31] G. Pellegrino, A. Vagati, P. Guglielmi, and B. Boazzo, "Performance comparison between surface-mounted and interior PM motor drives for electric vehicle application," *IEEE Transactions on Industrial Electronics,* vol. 59, no. 2, pp. 803-811, 2012.
[32] F. Magnussen, P. Thelin, and C. Sadarangani, "Performance evaluation of permanent magnet synchronous machines with concentrated and distributed windings including the effect of field-weakening," in *Second International Conference on Power Electronics, Machines and Drives (PEMD 2004)*, vol.2, pp. 679-685, 2004.
[33] A. M. El-Refaie, and T. M. Jahns, "Optimal flux weakening in surface PM machines using fractional-slot concentrated windings," *IEEE Transactions on Industry Applications,* vol. 41, no. 3, pp. 790-800, 2005.
[34] A. M. El-Refaie, and T. M. Jahns, "Scalability of surface PM Machines with concentrated windings designed to achieve wide speed ranges of constant-power operation," *IEEE Transactions on Energy Conversion,* vol. 21, no. 2, pp. 362-369, 2006.
[35] J. Cros and P. Viarouge, "Synthesis of high performance PM motors with concentrated windings," *IEEE Transactions on Energy Conversion,* vol. 17, no. 2, pp. 248-253, 2002.
[36] N. Bianchi and E. Fornasiero, "Impact of MMF Space harmonic on rotor losses in fractional-slot permanent-magnet machines," *IEEE Transactions on Energy Conversion,* vol. 24, no. 2, pp. 323-328, 2009.
[37] T. M. Jahns, G. B. Kliman, and T. W. Neumann, "Interior permanent-magnet synchronous motors for adjustable-speed drives," *IEEE Transactions on Industry Applications,* vol. IA-22, no. 4, pp. 738-747, 1986.
[38] T. Finken, M. Hombitzer, and K. Hameyer, "Study and comparison of several permanent-magnet excited rotor types regarding their applicability in electric vehicles," in *2010 Emobility - Electrical Power Train*, pp. 1-7, 2010.
[39] J. K. Tangudu, and T. M. Jahns, "Comparison of interior PM machines with concentrated and distributed stator windings for traction applications," in *2011 IEEE Vehicle Power and Propulsion Conference*, pp. 1-8, 2011.
[40] A. M. El-Refaie, "Fractional-slot concentrated-windings synchronous permanent magnet machines: opportunities and challenges," *IEEE Transactions on Industrial Electronics,* vol. 57, no. 1,pp. 107-121, 2010.
[41] X. Chen, J. Wang, V. I. Patel, and P. Lazari, "A nine-phase 18-slot 14-pole interior permanent magnet machine with low space harmonics for electric vehicle applications," *IEEE Transactions on Energy Conversion,* vol. 31, no. 3, pp. 860-871, 2016.
[42] G. Dajaku, "Elektrische maschine," German Patent, DE 10 2008 051 047 A1, 2010.
[43] G. Dajaku, and D. Gerling, "A novel 24-slots/10-poles winding topology for electric machines," in *IEEE International Electric Machines & Drives Conference (IEMDC)*, pp. 65-70, 2011.
[44] V. I. Patel, J. Wang, W. Wang, and X. Chen, "Analysis and design of 6-phase fractional slot per pole per phase permanent magnet machines with low space harmonics," in *2013 International Electric Machines & Drives Conference*, 2013, pp. 386-393.
[45] V. I. Patel, J. Wang, W. Wang, and X. Chen, "Six-phase fractional-slot-per-pole-per-phase permanent-magnet machines with low space harmonics for electric vehicle application," *IEEE Transactions on Industry Applications,* vol. 50, no. 4, pp. 2554-2563, 2014.
[46] J. Wang, V. I. Patel, and W. Wang, "Fractional-slot permanent magnet brushless machines with low space harmonic contents," *IEEE Transactions on Magnetics,* vol. 50, no. 1, pp. 1-9, 2014.
[47] P. B. Reddy, K. K. Huh, and A. M. E. Refaie, "Generalized approach of stator shifting in interior permanent-magnet machines equipped with fractional-slot concentrated windings," *IEEE Transactions on Industrial Electronics,* vol. 61, no. 9, pp. 5035-5046, 2014.
[48] A. S. Abdel-Khalik, S. Ahmed, and A. M. Massoud, "A

six-phase 24-slot/10-pole permanent-magnet machine with low space harmonics for electric vehicle applications," *IEEE Transactions on Magnetics,* vol. 52, no. 6, pp. 1-10, 2016.
[49] G. Dajaku and D. Gerling, "A novel tooth concentrated winding with low space harmonic contents," in *2013 International Electric Machines & Drives Conference*, pp. 755-760, 2013.
[50] G. Dajaku, H. Hofmann, F. Hetemi, X. Dajaku, W. Xie, and D. Gerling, "Comparison of two different IPM traction machines with concentrated winding," *IEEE Transactions on Industrial Electronics,* vol. 63, no. 7, pp. 4137-4149, 2016.
[51] A. S. Abdel-Khalik, S. Ahmed, and A. M. Massoud, "Low space harmonics cancelation in double-layer fractional slot winding using dual multiphase winding," *IEEE Transactions on Magnetics,* vol. 51, no. 5, pp. 1-10, 2015.
[52] X. Chen, J. Wang, and V. I. Patel, "A generic approach to reduction of magnetomotive force harmonics in permanent-magnet machines with concentrated multiple three-phase windings," *IEEE Transactions on Magnetics,* vol. 50, no. 11, pp. 1-4, 2014.
[53] M. V. Cistelecan, F. J. T. E. Ferreira, and M. Popescu, "Three phase tooth-concentrated multiple-layer fractional windings with low space harmonic content," in *IEEE Energy Conversion Congress and Exposition*, pp. 1399-1405, 2010.
[54] M. V. Cistelecan, F. J. T. E. Ferreira, and M. Popescu, "Three phase tooth-concentrated interspersed windings with low space harmonic content," in *The XIX International Conference on Electrical Machines - ICEM 2010*, pp. 1-6, 2010.
[55] A. S. Abdel-Khalik, S. Ahmed, and A. M. Massoud, "Effect of multilayer windings with different stator winding connections on interior PM machines for EV applications," *IEEE Transactions on Magnetics,* vol. 52, no. 2, pp. 1-7, 2016.
[56] G. Dajaku, "Elektrische maschine," German Patent, DE 10 2008 057 349 B3, 2010.
[57] G. Dajaku, and D. Gerling, "Eddy current loss minimization in rotor magnets of PM machines using high-efficiency 12-teeth/ 10-slots winding topology," in *2011 International Conference on Electrical Machines and Systems*, pp. 1-6, 2011.
[58] G. Dajaku, W. Xie, and D. Gerling, "Reduction of low space harmonics for the fractional slot concentrated windings using a novel stator design," *IEEE Transactions on Magnetics,* vol. 50, no. 5, pp. 1-12, 2014.

Xiao Chen received B.Eng. degree in electrical engineering from Harbin Institute of Technology at Weihai, Weihai, China, in 2009, M.Eng. degree in electrical engineering from Harbin Institute of Technology, Harbin, China, in 2011, and Ph.D degree from University of Sheffield, Sheffield, UK in 2015 respectively. He is currently a research associate in Dept. of Electronic and Electrical Engineering, University of Sheffield, UK. His current research interests include the modeling, design and analysis of permanent-magnet synchronous machines for traction applications.

Jiabin Wang received the B.Eng. and M.Eng. degrees from Jiangsu University of Science and Technology, Zhenjiang, China, in 1982 and 1986, respectively, and the Ph.D. degree from the University of East London, London, U.K., in 1996, all in electrical and electronic engineering.

Currently, he is a Professor in Electrical Engineering at the University of Sheffield, Sheffield, U.K. From 1986 to 1991, he was with the Department of Electrical Engineering at Jiangsu University of Science and Technology, where he was appointed a Lecturer in 1987 and an Associated Professor in 1990. He was a Postdoctoral Research Associate at the University of Sheffield, Sheffield, U.K., from 1996 to 1997, and a Senior Lecturer at the University of East London from 1998 to 2001. His research interests range from motion control and electromechanical energy conversion to electric drives for applications in automotive, renewable energy, household appliances and aerospace sectors.

He is a fellow of the IET and a senior member of IEEE.